Vacuum 84 (2010) 13–18

Contents lists available at ScienceDirect

Vacuum

journal homepage: www.elsevier.com/locate/vacuum

On the origin of Ru bilayer island growth on Pt(111)

A. Bergbreiter, A. Berkó [1], P.M. Erne, H.E. Hoster*, R.J. Behm*

Institute of Surface Chemistry and Catalysis, Ulm University, D-89069 Ulm, Germany

Keywords:
Scanning tunnelling microscopy
Epitaxial growth
Bilayer island growth
Ruthenium
Platinum

A B S T R A C T

Depending on the growth temperature, Ru growth on Pt(111) proceeds preferentially via nucleation and growth of bilayer islands [Hoster HE, Iwasita T, Baumgärtner H, Vielstich W. Phys Chem Chem Phys 2001;3:337]. The physical origin for this growth behaviour was investigated by scanning tunnelling microscopy. The role of the lattice mismatch is elucidated by comparing Ru growth on Pt(111) with that on a pseudomorphic Pt monolayer film on an Ru(0001) substrate, where lattice misfit is absent. The results are interpreted using existing concepts on the adsorption properties of bimetallic surfaces, the consequences of our results and our mechanistic interpretation on the understanding of bilayer island growth in metal-on-metal epitaxy in general are discussed.

1. Introduction

Nucleation, growth, and structure of ultra-thin metal films have attracted considerable attention in recent years, not only because of the fundamental interest in the atomic scale understanding of structure formation and growth processes [1,2], but also because of their use as model systems for studies of the relation between structure and functional properties of bimetallic surfaces, e.g., in the fields of magnetism [3] or (electro-)catalysis [4]. In this paper, which is part of a comprehensive study on the surface chemistry of structurally well-defined bimetallic PtRu surfaces (see, e.g., refs. [5–9]), we present results on the growth of Ru on Pt(111). PtRu surfaces are of particular interest due to the use of PtRu as state-of-the-art anode catalyst in low-temperature polymer electrolyte fuel cells (PEFCs) [10], and therefore structurally well-defined Ru modified Pt(111) surfaces would be another interesting model system, in addition to the Ru(0001) based Pt/Ru(0001) and PtRu/Ru(0001) surfaces investigated previously (see above).

In a previous study, it was reported that Ru islands vapour-deposited on Pt(111) at about 80–100 °C predominantly adopt a height of two atomic layers [11], very similar to the behaviour observed for Co/Pd(111) [12,13], Co/Cu(111) [14], Co/Au(111) [15,16], and Co/Ag(111) [16]. For the bimetallic systems Co/Au(111) and Co/Pd(111), the lattice misfit between host and guest metal was suggested to be the main reason for the observed bilayer island growth [13,15], whereas in another study the stronger Co–Co bond compared to the Pd–Co bond was proposed as a considerable contribution to the driving force for the bilayer island growth of Co/Pd(111) [12]. For Ru/Pt(111), the lattice mismatch is about 2.6% (nearest neighbour distance: Ru–Ru = 0.27 nm, Pt–Pt = 0.277 nm) and could therefore have significant effects on the growth behaviour. On the other hand, Pt and Ru are very different with respect to their chemical properties, which include significant differences between Ru–Pt, Ru–Ru and Pt–Pt bonds [7,17].

In the present paper, we are particularly interested in unravelling the role of the lattice misfit and lattice misfit-related effects in the Ru bilayer island growth on Pt(111). This is done by comparing the growth of Ru on Pt(111) and on strained Pt monolayer films grown pseudomorphically on an Ru(0001) substrate. These strained Pt films have the same lattice constant as Ru(0001), and therefore there is no lattice mismatch for subsequent growth of Ru on this Pt monolayer. The results are interpreted using existing concepts on the adsorption properties of bimetallic surfaces. The consequences of our results and our mechanistic interpretation on the understanding of bilayer island growth in metal-on-metal epitaxy in general are discussed.

2. Experimental

The surfaces were prepared and characterized in an ultrahigh vacuum (UHV) system with a base pressure of 6×10^{-11} mbar, equipped with two electron beam evaporators (Omicron EFM 3) for Ru and Pt deposition, a quadrupole mass spectrometer for residual gas analysis, a home-built pocket-size scanning tunnelling microscope (STM) and an Auger-electron spectrometer (AES) (Perkin

* Corresponding authors.
E-mail addresses: harry.hoster@uni-ulm.de (H.E. Hoster), juergen.behm@uni-ulm.de (R.J. Behm).
[1] Perm. address: Reaction Kinetics Research Laboratory, Institute of Nanochemistry and Catalysis, Chemical Research Center of the Hungarian Academy of Sciences, University of Szeged, H-6720 Szeged, Dóm tér 7, Hungary.

0042-207X/$ – see front matter © 2009 Elsevier Ltd. All rights reserved.
doi:10.1016/j.vacuum.2009.04.001

Elmer CMA 10-155) for sample characterization. Further details are given in ref. [18]. Clean Ru(0001) substrates were prepared by ion bombardment (0.5 keV Ar^+, ca. 5 μA Ar^+ ion beam) followed by three annealing cycles up to 1650 K. This was followed by exposure to 1 Langmuir ($10\,s \times 10^{-7}$ mbar) O_2 during cool-down below 800 K, and two final flash annealings to 1650 K to remove carbon contaminations and adsorbed oxygen. Cleaning of Pt(111) also started with Ar^+ ion bombardment (conditions as for Ru(0001) cleaning), which was followed by three annealing cycles to 1100 K and subsequent oxygen adsorption (1 L O_2, conditions similar as for Ru(0001)). Finally, the sample was annealed to 1050 K at controlled annealing/cooling rates of 4 K s^{-1}/2 K s^{-1}. After this treatment, the contaminations of the two substrates were below the AES detection limit, and STM images revealed atomically smooth, large terraces (terrace width ~ 50–200 nm). Pt and Ru were deposited at rates of 0.03–0.1 ML min^{-1}, the respective sample temperatures are given in the text. During deposition, the pressure remained below 6×10^{-10} mbar.

3. Results and discussion

Fig. 1a shows the morphology of a Pt(111) surface after deposition of 0.67 monolayers (1 ML = 1 adlayer atom per surface atom) Ru at 310 K (deposition rate: 0.1 ML min^{-1}). The Pt(111) surface is homogeneously covered by islands, whose shape varies between relaxed triangular and hexagonal. The island density and the mean diameter of the islands are ~0.008 nm^{-2}, and ~1–6 nm, respectively, in agreement with earlier data [19]. The amount of bilayer Ru islands is much higher than expected, which also resembles previous findings [11]. If the sample is annealed to 400 K after deposition (Fig. 1b), this trend becomes even more pronounced. Now almost all islands have heights of two atomic layers (see also the line profiles shown as insets in Fig. 1), with the second layer fully covering the first layer. In addition, the islands adopt a preferentially triangular shape with a uniform orientation. The island shape and orientation closely resemble those reported for Pt homoepitaxy on Pt(111) [20] or Pt growth on Ru(0001) [7,21]; they are indicative for a uniform stacking (fcc or hcp) of all islands with respect to the substrate. Based on our data, however, it is not possible to decide which of the two stacking types is adopted. The bilayer island density is ~0.01 nm^{-2}, which is essentially identical to that before annealing. Therefore, Ru mass transport occurs exclusively within each island, transport between different islands is not yet activated. Hence, the subsequent annealing step, where the temperature is raised by 90 K only, not only increases the mobility of Ru adatoms at the island edge to energetically optimize the lateral shape of the islands, but is sufficient also to activate an interlayer mass transport of Ru adatoms from the first to the second atomic layer. In an atomistic picture, the driving force for a single Ru atom to 'climb' into the second layer could result i) from a higher binding energy of a Ru adatom on Ru islands compared to Ru adsorption on Pt(111) or ii) from interactions between the Ru adatoms, e.g., due to a lattice mismatch, which effectively limit the size of the islands and favour a vertical growth once a critical island size is reached.

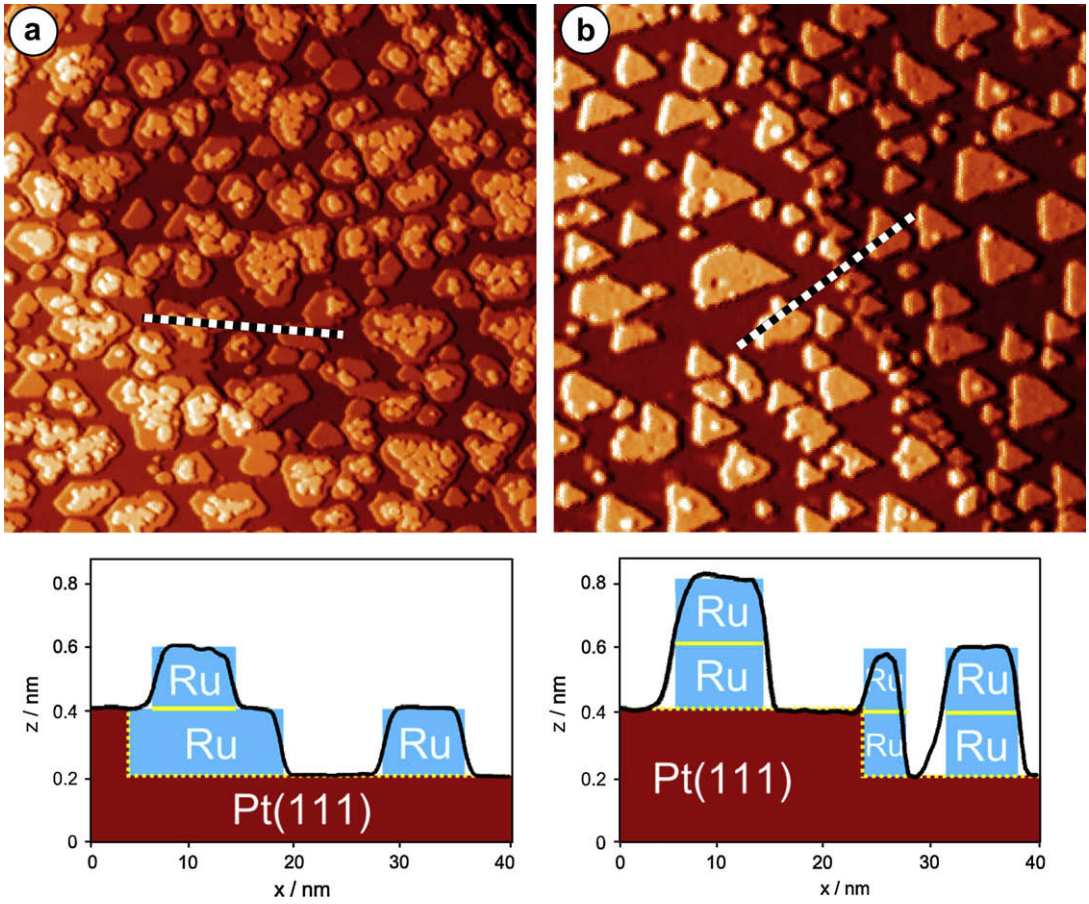

Fig. 1. Large scale STM images (top) and schematic height profiles (bottom) of a Pt(111) surface (a) after deposition of 0.67 ML Ru at 310 K (100 × 100 nm^2, $I_t = 0.3$ nA, $U_t = 1.3$ V) and (b) after deposition of 0.65 ML Ru at 300 K (100 nm × 100 nm, $I_t = 0.9$ nA, $U_t = 0.5$ V) followed by annealing to 400 K. The height profiles shown in the bottom are measured along the black–white lines indicated in the STM images.

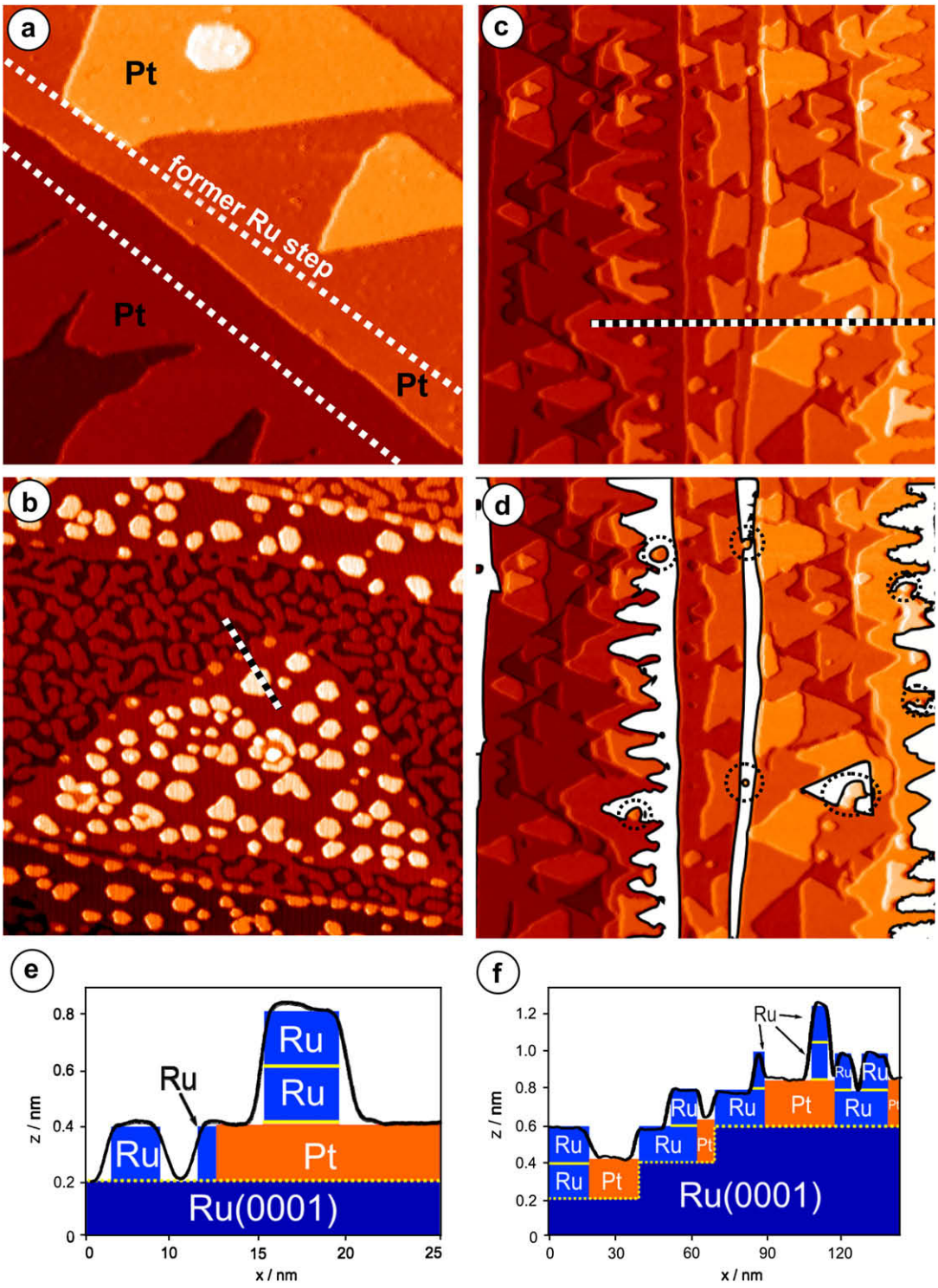

Fig. 2. Large scale STM images (top and middle) and schematic height profiles (bottom) of a Ru(0001) surface (a) after deposition of 0.42 ML Pt at 600 K (200 nm × 200 nm, $I_t = 0.3$ nA, $U_t = 1.7$ V); (b) after subsequent deposition of 0.54 ML Ru at 600 K on the Pt/Ru(0001) surface shown in (a). (c) and (d) show the morphology of a Ru/Pt/Ru(0001) surface prepared by deposition of 0.2 ML Pt ($T_{dep} = 600$ K, 0.03 ML min^{-1}) and subsequent deposition of 1.2 ML Ru ($T_{dep} = 300$ K, 0.1 ML min^{-1}), followed by annealing to 500 K (200 × 200 nm^2, $I_t = 0.3$ nA, $U_t = 1.7$ V). The exposed Pt areas are marked white in (d). (e), (f): schematic height profiles measured along the black-and-white lines in the images in (b) and (c).

As mentioned in the Introduction, the influence of the lattice mismatch between Ru and Pt on the growth process and hence on the resulting growth morphology can be "switched off" by using a Pt film pseudomorphically grown on Ru(0001) as substrate for the subsequent Ru vapour deposition. The resulting growth behaviour is illustrated in Fig. 2. Fig. 2a shows the morphology of a 0.42 ML Pt film grown on Ru(0001) at 600 K (deposition rate: 0.04 ML min^{-1}). The higher deposition temperature was used to produce larger Pt islands for the subsequent Ru deposition step. Under these conditions, Pt deposition results in large triangular monolayer islands on

the terraces, and Pt stripes attached to the ascending steps of the Ru(0001) substrate. In the STM image in Fig 2a, a narrow terrace passes diagonally through the imaged area, where Pt only forms a step decorating stripe and no islands. The positions of the former Ru steps are marked in the image. The triangular shape of the islands and the step decorations on the larger terraces fit to previous STM observations of the same system [7,21,22]. The island in the upper left corner appears truncated at its lower left corner, with the truncation line coinciding with the position of the underlying Ru step. This growth behaviour, which was reproducibly observed wherever a Pt island tried to overgrow a former Ru step and hence continue growing on a Pt cover layer rather than on the Ru(0001) substrate, reflects a preference of Pt atoms to occupy Ru rather than Pt sites and thus a higher interaction between Pt and Ru than between the strained Pt layer and Pt, which fully agrees with previous conclusions [7].

Deposition of Ru on the partly Pt monolayer covered Ru(0001) surface (Pt_{ML}/Ru(0001)) at 300 K gives rise to a rather high density of Ru monolayer islands on the Ru(0001) substrate, pointing to a rather low mobility of Ru on the Ru(0001) substrate [2]. Under these conditions, Ru islands are formed also on large Pt monolayer islands. This is illustrated in Fig. 2b, which shows a partly Pt pre-covered Ru(0001) surface (0.42 ML, $T_{dep} = 600$ K, 0.04 ML min^{-1}) after subsequent deposition of 0.54 ML Ru at 300 K, followed by annealing to 500 K. (It should be noted that, based on high resolution STM images, exchange of Pt and Ru deposit atoms can be excluded under these conditions.) As schematically shown in the height profile in Fig. 2e, the Ru islands on the Pt monolayer island are generally ~0.4 nm high, i.e., they represent bilayer islands.

Deposition of Ru on the Pt/Ru(0001) surface at 600 K leads to the morphology illustrated in Fig. 2c. For better visibility, Fig. 2d shows the same STM image with the Pt areas marked white. Also under these conditions, we have no indications of Pt–Ru exchange. The preference of the Pt islands to form $\{10\bar{1}0\}$ oriented steps results in stripes of Pt attached to the ascending Ru steps which alternately exhibit zig-zag shaped and straight steps. These Pt monolayer stripes are visible as slightly depleted areas. The Ru atoms post-deposited on the partly Pt pre-covered surface are almost exclusively found on Pt-free areas of the Ru(0001) substrate, the few Ru islands on top of Pt monolayer islands are marked by white circles. This gives rise to a line of second or even third layer Ru in the vicinity of the Pt decorations or islands, whereas on the larger, Pt uncovered areas Ru mainly forms a monolayer film. Close to its right end, the height profile in Fig. 2f runs over a Pt island, where it passes also over a Ru island. This Ru island, and also all other Ru islands on the Pt covered areas, has a height of two atomic layers, similar to the Ru islands on Pt(111) (see Fig. 1b).

In Fig. 3, we compare the amounts of Ru adsorbed on the Pt monolayer areas and on the Pt-free areas after deposition of different amounts of Ru on the surface shown in Fig. 2a at 300 K, followed by annealing to 500 K. The experiment was performed by moving the sample slowly out of the Ru beam during Ru deposition, which results in a gradient of the Ru coverage along the surface. The morphology of the resulting surface was investigated in a number of areas with different Ru coverages, for each area we analyzed 0.05 μm^2. Obviously, the Ru coverages in the Pt monolayer covered and Pt-free areas are identical in all cases. This result can be explained by the relatively low adatom mobilities on both areas at the deposition temperature of 300 K, which give rise to rather higher island densities, both on the bare Ru area and on the Pt monolayer covered areas [2]. These islands are largely stable against dissolution at the annealing temperature of 500 K. On the other hand, annealing to 500 K is sufficient to activate Ru interlayer mass transport at each Ru island on the Pt monolayer covered areas, resulting in the perfect bilayer shape of the Ru islands on these areas (see above).

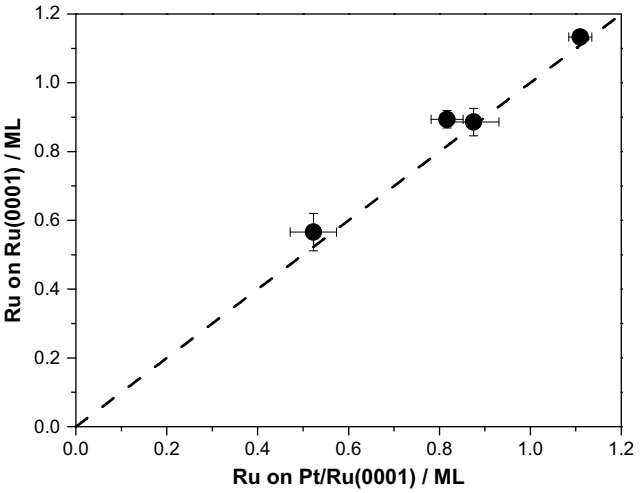

Fig. 3. Plot of the distribution of Ru islands after Ru deposition (deposition temperature/rate 600 K/0.1 ML min^{-1}) on a Ru(0001) surface pre-covered with Pt monolayer islands shown in Fig. 2a. The ordinate shows the amount of Ru grown on the bare Ru(0001) substrate, the abscissa the amount of Ru on the Pt monolayer islands.

Next, we analyzed the amounts of Ru in the 1st, 2nd, and 3rd layer of the Ru islands on the Ru(0001) substrate (Fig. 4a) and on the Pt monolayer covered areas (Fig. 4b), respectively. They are plotted as a function of the total Ru coverage in the analyzed area in Fig. 4. Below $\theta_{Ru} \approx 0.8$ ML, there are virtually no bilayer Ru islands in the Pt-free areas. It should be noted that the amount of 2nd layer Ru is not markedly higher without the annealing step to 500 K, which means that Ru homoepitaxy on Ru(0001) proceeds in a layer-by-layer growth mode and that this is kinetically feasible already for deposition at 300 K. Thermodynamically, a layer-by-layer ('Frank-van der Merwe') growth mode is expected for homoepitaxial growth; kinetically, a relatively perfect layer-by-layer growth means that the barrier for a Ru adatom to pass over a descending step ('Ehrlich–Schwoebel (ES) barrier' [23,24]) is small enough to be overcome at room temperature. This growth behaviour closely resembles that for Pt homoepitaxy on Pt(111) [20], while on other fcc(111) surfaces, e.g., for Ag homoepitaxy on Ag(111), high ES barriers lead to a distinct mound formation [25]. On the Pt monolayer covered areas, on the other hand, the islands predominantly adopt a height of two atomic layers, similar to the growth behaviour on Pt(111) (see Fig. 1). Although nucleation and growth processes and hence also the formation of the Ru islands are kinetically controlled, the increasing tendency for Ru bilayer island formation upon annealing clearly indicates that the bilayer islands represent the thermodynamically stable configuration and that their formation is kinetically hindered during Ru deposition at room temperature. Otherwise, annealing would favour dissolution of the second layer islands. Our data furthermore indicate, that Ru interlayer mass transport is activated without Ru mass transport between Ru islands or between Pt monolayer islands and bare Ru(0001) areas.

The driving force for the distinct non-2D growth of Ru on Pt (Pt(111) or Pt_{ML}/Ru(0001)) must be a significantly higher energy for Ru–Ru bonding than for Ru–Pt bonds. This is reflected also by the impurity segregation energies of Pt in Ru and Ru in Pt [26], which favour Pt rather than Ru in the outermost layer. This condition is not sufficient, however, to rationalize the particular stability of bilayer islands rather than multilayer islands. The latter requires an additional stabilization of the second Ru layer on a Pt surface in contrast to third and higher Ru layers. The specific stabilization of the second Ru layer can be explained by vertical

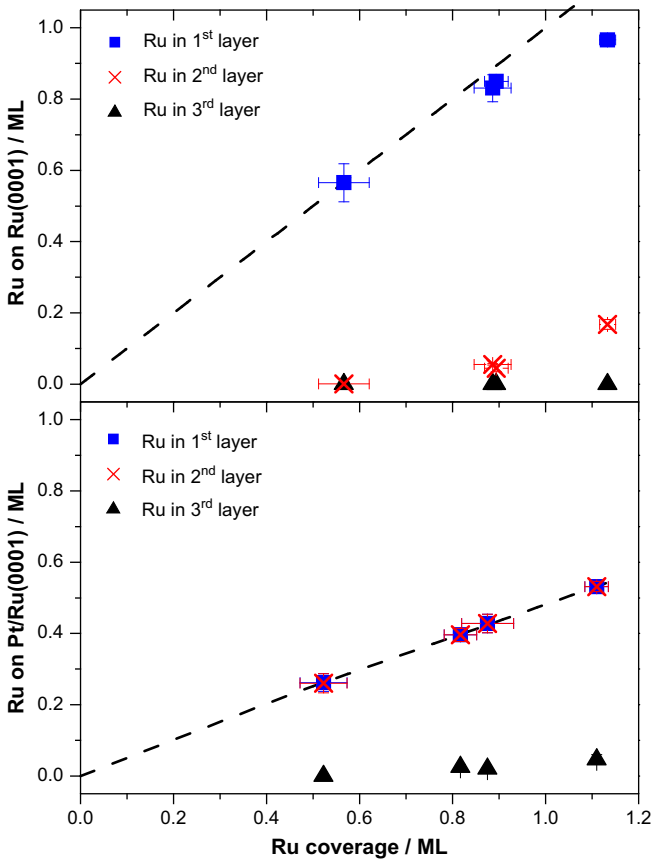

Fig. 4. Amount of Ru in the 1st, 2nd and 3rd layer as a function of the Ru coverage on the surfaces studied in Fig. 3. Upper graph: Ru on Ru(0001) terraces, the dashed line indicates the first Ru layer population if all Ru were in the 1st layer; lower graph: Ru on Pt islands, the dashed line indicates the first Ru layer population for ideal bilayer islands.

ligand effects, in this case by the specific interaction between Ru deposit layer and Pt substrate layer [17]. Due to the weaker bonding between Pt and Ru compared to Ru and Ru, we expect the adsorption power of the (first) Ru layer on Pt to be higher than that of a Ru layer on a Ru substrate ('conservation of bond order'), opposite to the distinct loss in adsorption power of a Pt monolayer on a Ru(0001) substrate relative to Pt(111) [5,6,17,21]. This means, that the binding of Ru to a Ru monolayer on Pt(111) is not only stronger than to Pt(111) itself, but also stronger than to thicker Ru layers. If the substrate is a Pt monolayer on Ru(0001), the Pt atoms are more strongly bound to the Ru substrate than on Pt(111). This in turn reduces their bonding power significantly and results in an even weaker bond to Ru adislands than obtained on bulk Pt(111). This way, the even more pronounced tendency for Ru bilayer island formation on Pt/Ru(0001) than on Pt(111) can be explained straightforwardly.

The above explanation of the driving force for bilayer island growth, which is based on existing concepts on the adsorption properties of bimetallic surfaces, is proposed to be generally valid for metal-on-metal epitaxy. Accordingly, bilayer island growth is expected for systems where on the one hand the interaction between the deposit material is higher than that between deposit and substrate, but where on the other hand the interaction between second and third island layer is sufficiently weakened, as a result of the stronger (weaker) interaction between first layer (substrate) and second layer (first layer), to make the population of the third layer energetically less favorable than the formation of larger bilayer islands. Examples for such kind of growth include a number of Co/metal systems [12–16]. Because of the rapidly decreasing size of the energetic variations in the interaction between subsequent layers [17], the preferential formation of trilayer or thicker islands is very unlikely.

4. Conclusions

We have shown in a detailed STM study that the bilayer growth behaviour of Ru on Pt(111) results from the combination of two effects: i) a weaker binding of Ru adatoms to the underlying Pt substrate than to Ru island atoms is responsible for multilayer island formation and hence minimizing the Ru/Pt interface; ii) the weaker interaction between Pt(111) substrate and Ru first layer islands compared to Ru–Ru interactions results in a stronger Ru–Ru interaction between first and second layer in Ru islands compared to Ru–Ru bulk interactions and correspondingly a weaker interaction between second and third Ru island layer. This in turn results in a preferential stabilization of bilayer Ru islands. Effects related to the lattice misfit between Pt(111) substrate and Ru play no major role as physical origin for the bilayer growth behaviour; for (unstrained) Ru deposition on a (strained) Pt monolayer on Ru(0001), the bilayer growth is even more pronounced. In analogy to the observed and calculated lower adsorption strength of Pt_{ML}/Ru(0001) compared to Pt(111) this gives rise to a weaker Ru–Pt bonding and hence to even stronger (weaker) Ru–Ru interactions between first and second (second and third) Ru layer in Ru islands. This schematic explanation, which agrees fully with the calculated segregation energies for the preferential surface segregation of Pt from PtRu alloys or Pt impurities in Ru, is proposed as a general scheme for the driving force for bilayer island growth.

Acknowledgements

This work was supported by the Landesstiftung Baden-Württemberg, within the Competence Network Functional Nanostructures. Furthermore, we gratefully acknowledge support by the Alexander von Humboldt foundation for A. Berkó.

References

[1] Brune H. Surf Sci Rep 1998;31:121.
[2] Venables JA. Surf Sci 1994;299–300:798.
[3] Shen J, Kirschner J. Surf Sci 2002;500:300.
[4] Chen JG, Menning CA, Zellner MB. Surf Sci Rep 2008;63:201.
[5] Rauscher H, Hager T, Diemant T, Hoster H, Buatier de Mongeot F, Behm RJ. Surf Sci 2007;601:4608.
[6] Diemant T, Rauscher H, Behm RJ. J Phys Chem C 2008;112:8381.
[7] Hoster HE, Bergbreiter A, Erne P, Hager T, Rauscher H, Behm RJ. Phys Chem Chem Phys 2008;10:3812.
[8] Hoster HE, Behm RJ. The effect of structurally well-defined Pt modification on the electrochemical and electrocatalytic properties of Ru(0001) electrodes. In: Koper MTM, editor. Fuel cell catalysis: a surface science approach. Chichester: Wiley & Sons; 2008. p. 459.
[9] Behm RJ. Z Phys Chem 2009;223:9.
[10] Peppley BA, Amphlett JC, Mann RF. Catalyst development and kinetics for methanol fuel processing. In: Vielstich W, Lamm A, Gasteiger HA, editors. Handbook of fuel cells – fundamentals technology and applications. Fuel cells and technology, vol. 3. Chichester: Wiley; 2003. p. 131.
[11] Hoster HE, Iwasita T, Baumgärtner H, Vielstich W. Phys Chem Chem Phys 2001;3:337.
[12] Wasniowska M, Janke-Gilman N, Wulfhekel W, Przybylski M, Kirschner J. Surf Sci 2007;601:3073.
[13] Wasniowska M, Wulfhekel W, Przybylski M, Kirschner J. Phys Rev B 2008;78:035405.
[14] de la Figuera J, Prieto JE, Ocal C, Miranda R. Surf Sci 1994;307:538.
[15] Voigtländer B, Meyer G, Amer NM. Phys Rev B 1991;44:10354.
[16] Morgenstern K, Kibsgaard J, Lauritsen JV, Laesgaard E, Besenbacher F. Surf Sci 2007;601:1967.
[17] Schlapka A, Lischka M, Gross A, Käsberger U, Jakob P. Phys Rev Lett 2003;91:016101.

[18] Kopatzki E, Behm RJ. Surf Sci 1991;245:255.
[19] Iwasita T, Hoster H, John-Anacker A, Lin W-F, Vielstich W. Langmuir 2000;16:522.
[20] Bott M, Michely T, Comsa G. Surf Sci 1992;272:161.
[21] Buatier de Mongeot F, Scherer M, Gleich B, Kopatzki E, Behm RJ. Surf Sci 1998;411:249.
[22] Schlapka A, Käsberger U, Menzel D, Jakob P. Surf Sci 2002;502–503:129.
[23] Ehrlich G, Hudda FG. J Chem Phys 1966;44:1039.
[24] Schwoebel RL, Shipsey EJ. J Appl Phys 1966;37:3682.
[25] Vrijmoeth H, van der Vegt HA, Meyer JA, Vlieg E, Behm RJ. Phys Rev Lett 1994;72:3843.
[26] Ruban AV, Skriver HL, Nørskov JK. Phys Rev B 1999;59:15990.